Biol. Cybern. 84, 411–423 (2001)

Biological Cybernetics

A computational model of action selection in the basal ganglia. II. Analysis and simulation of behaviour

K. Gurney, T. J. Prescott, P. Redgrave

Department of Psychology, University of Sheffield, Sheffield S10 2TP, UK

Received: 16 July 2000 / Accepted in revised form: 30 October 2000

Abstract. In a companion paper a new functional architecture was proposed for the basal ganglia based on the premise that these brain structures play a central role in behavioural action selection. The current paper quantitatively describes the properties of the model using analysis and simulation. The decomposition of the basal ganglia into selection and control pathways is supported in several ways. First, several elegant features are exposed – capacity scaling, enhanced selectivity and synergistic dopamine modulation – which might be expected to exist in a well designed action selection mechanism. The discovery of these features also lends support to the computational premise of selection that underpins our model. Second, good matches between model globus pallidus external segment output and globus pallidus internal segment and substantia nigra reticulata area output, and neurophysiological data, have been found which are indicative of common architectural features in the model and biological basal ganglia. Third, the behaviour of the model as a signal selection mechanism has parallels with some kinds of action selection observed in animals under various levels of dopaminergic modulation.

1 Introduction

In Gurney et al. (2001), henceforth referred to as GPR1, we proposed a new functional architecture for the basal ganglia based on the computational premise that these structures perform a selection function with respect to behavioural control. It was shown that, given this functional interpretation, the processing intrinsic to the basal ganglia may be viewed as one of signal selection. This was defined formally and it was claimed that the basal ganglia met the criteria to perform useful signal selection. The current paper articulates our model quantitatively and validates this claim by demonstrating analytically its selection-mechanistic behaviour. Further we show in simulation how the model is consistent with certain neurobiological data, and that dopaminergic modulation in the model endows it with selection properties consistent with behavioural change under dopamine depletion or excess.

The plan of the paper is as follows. Section 2 gives details of the computational model based on the new basal ganglia functional architecture described in GPR1. We then solve the model analytically for the individual nucleus activities at equilibrium (Sect. 3.1) and go on to use these solutions to obtain general results about the selection behaviour of the model in toto (Sect. 3.2). The analysis is completed with an examination of the effects of dopaminergic regulation (Sect. 3.3). The main analytic results are then demonstrated in simulation (Sect. 4), which is also used to show similarities between the model's dynamic behaviour and corresponding physiological data when presented with large, short-duration input stimuli.

2 Quantifying the new functional architecture

For a synoptic reference throughout this section, Fig. 1 shows the structure of a single channel annotated with each of the model parameters. We first describe the general artificial neural model and go on to give an account of each nucleus in turn.

2.1 General neural framework

The model uses artificial neurons of the leaky-integrator type (Arbib 1995). This is the simplest neural model which incorporates the idea of a dynamic membrane potential while obviating the need to model an abundance of ionic channels (Yamada et al. 1989). As such, it is a common choice for biologically plausible models of

Correspondence to: K. Gurney
(e-mail: k.gurney@shef.ac.uk)

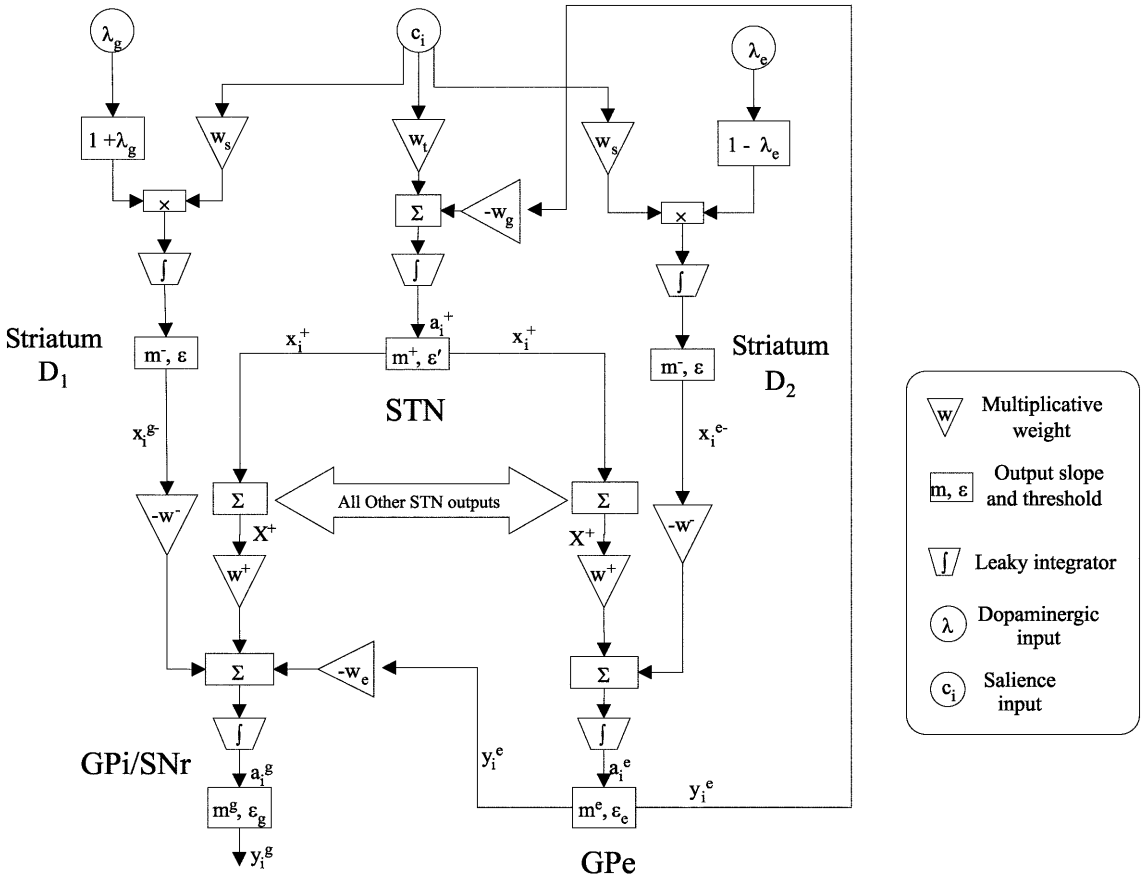

Fig. 1. Model details and parameters (one channel only)

neural circuits. The leaky integrator is defined by the rate of change of an activation a which may be interpreted as the membrane potential near the axon hillock. Let u be the total post-synaptic potential generated by the afferent input, k a rate constant which depends on the cell membrane capacitance and resistance, and $\tilde{a}$ the equilibrium activation then

$$\dot{a} = -k(a - u)$$
$$\tilde{a} = u \tag{1}$$

where $\dot{a} \equiv \mathrm{d}a/\mathrm{d}t$. The output y of the neuron (supposed to correspond to the mean firing rate) is a monotonic increasing function of a. It will be bounded below by 0 and above by some maximum value $y_{\max}$ which may be normalised to 1. We adopt a piecewise linear output function of the form.

$$y = \begin{cases} 0 : & a < \epsilon \\ m(a - \epsilon) : & a \le \epsilon \le 1/m + \epsilon \\ 1 : & a > 1/m + \epsilon \end{cases} \tag{2}$$

The choice of this form for y (over the more usual logistic sigmoid) is motivated by the fact that the equilibrium behaviour of the model is then analytically tractable; the activation space of the model is divided into a set of disjoint regions whose individual behaviour is linear, and which may be determined exactly.

Under certain circumstances, it may be possible to ensure that y never reaches 1. It is then possible to write the output relation as

$$y = m(a - \epsilon)H(a - \epsilon) \tag{3}$$

where $H(\ )$ is the Heaviside step function. The assumption $y < 1$ is made for the purposes of the analytic solution of the model and is borne out in simulation.

2.2 Striatum

As discussed in GPR1, the striatal model admits the possibility of local recurrent inhibition but is not contingent on its operation. The recurrent network model which allows this consists of a set of leaky integrators described by (1) and (3). Within each recurrent net, each node is connected to every other by an inhibitory link with weight w^-. Let the non-zero slope in the output relation be m^-, the equilibrium output of the ith node x_i^-, and the output threshold ϵ, then the network equilibrium state is defined by the following set of coupled equations

$$\tilde{a}_i = J_i - w^- \sum_{j \neq i} x_j^-$$
$$x_i^- = m^-(\tilde{a}_i - \epsilon)H(\tilde{a}_i - \epsilon) \quad (4)$$

Now let $J_k = \max_i(J_i)$. If $w^- m^- \geq 1$, then one solution to (4) is

$$x_i^- = m^-(J_i - \epsilon)H(J_i - \epsilon)\delta_{ik} \quad (5)$$

where δ_{iK} is the Kronecker delta. This solution may be easily verified by direct substitution. At equilibrium, if $J_k > \epsilon$ there is a single node, k, which has non-zero output $x_k^- = m^-(J_k - \epsilon)$. If no input exceeds ϵ, then all nodes have zero output. In terms of the selection theory developed in GPR1, if x_k^- is greater than the selection threshold θ_2, then the net is perfectly decisive ($D(x) = 1$), minimally promiscuous with $\phi(x) = 1/n$ (for n channels) and implements hard switching.

To make contact with the idea of channel salience c_i as input, we put $J_i = w_s c_i$, where w_s is a measure of the overall synaptic efficiency of the medium spiny neurons in integrating its inputs. Striatum is supposed to consist of many recurrent nets of the type defined by (4), each processing several channels. The solution in (5) implies, however, that only those saliences which are maximal within each network are contenders for further processing. Now suppose there are N striatal networks and let c_{ri} be the salience on the ith channel of network r. Let $c_{rk(r)} = \max_i(c_{ri})$ and $P = \{c_{rk(r)} : r = 1, \ldots, N\}$, the set of *potentially active* channels. Now re-label each member of P with its network index so that each local recurrent network r obeys, at equilibrium, a relation of the form in (5) for its maximally salient channel

$$x_r^- = m^-(w_s c_r - \epsilon)H(c_r - \epsilon/w_s) \qquad r = 1, \ldots, N \quad (6)$$

Here, the step function has been written in such a way as to emphasise the dependence on the salience. The up-state/down-state behaviour of medium spiny cells is then modelled very simply by assigning a positive value to ϵ so that the transition from 'down' to 'up' state corresponds to the requirement of a minimum positive salience. In terms of selection, $\epsilon > 0$ ensures a primary filtering mechanism forcing all $x_i^- < \epsilon$ to be non-selected.

Now observe that the relation in (6) also describes the equilibrium output of a single neuron in isolation. The situation obtained after the local recurrent nets have relaxed to equilibrium is, therefore, formally identically to that obtained if there had been only N striatal channels ab initio.

2.2.1 Dopaminergic modulation. We now introduce the dopamine modulation of medium spiny cell activity. In principle, it would be desirable to model the dynamics of the dopamine levels resulting from striatal innervation by the substantia nigra compacta area (SNc) and, in particular, the short-latency dopamine signals associated with the onset of biologically significant stimuli (Schultz and Romo 1990). However, we limit ourselves to the simpler case of dealing with tonic or 'background' levels of dopamine that might alter as a result of pathologies of SNc, laboratory manipulations in animals or intoxicated states in humans. Further we assume that such tonic dopaminergic input to striatum is diffuse enough that it is essentially constant over all channels.

Dopaminergic synapses occur primarily on the shafts of the spines of medium spiny cells (Bouyer et al. 1984). This is suggestive of a multiplicative (rather than additive) process. However, irrespective of the details of the synaptic mechanism, it is always possible to model it phenomenologically by introducing a multiplicative factor in the synaptic strength w_s. In line with the observed properties of dopaminergic modulation discussed in GPR1, we assume excitatory effects (via D1 receptors) in the selection pathway and inhibitory effects (via D2 receptors) in the control pathway. Thus, for the control pathway, the afferent synaptic strength w_s is modified to $w_s(1 - \lambda_e)$, where λ_e parameterises the degree of tonic dopamine modulation in this pathway and $0 \leq \lambda_e \leq 1$. The step function in (6) now becomes $H[c_i - \epsilon/(w_s(1 - \lambda_e))]$. To ease notation and to emphasise that the step function determines the transition to the up state in a dopaminergic dependent way, we write it as $H_i^{\uparrow}(\lambda_e)$. The equilibrium output x_i^{e-} of striatal medium spiny cells in ith channel of the control pathway is now

$$x_i^{e-} = m^-[w_s(1 - \lambda_e)c_i - \epsilon]H_i^{\uparrow}(\lambda_e) \quad (7)$$

Similarly, for the selection pathway, w_s becomes $w_s(1 + \lambda_g)$, $0 \leq \lambda_g \leq 1$ so that if x_i^{g-} is the equilibrium output on the ith channel in this pathway

$$x_i^{g-} = m^-[w_s(1 + \lambda_g)c_i - \epsilon]H_i^{\uparrow}(-\lambda_g) \quad (8)$$

where $H_i^{\uparrow}(-\lambda_g) = H[c_i - \epsilon/w_s(1 + \lambda_g)]$.

Let P_e^*, $P_g^* \subset P$ be the sets of channels which have active (non-zero) striatal outputs in the control and selection pathways, respectively. Now, $H_i^{\uparrow}(-\lambda_g) \geq H_i^{\uparrow}(\lambda_e)$ so that $P_e^* \subseteq P_g^*$ with equality in both relations holding only if $\lambda_e = \lambda_g = 0$. We will therefore refer to the set of *active channels* $P^* = P_g^*$, which is the set of channels associated with non-zero striatal output in both pathways.

2.3 Subthalamic nucleus (STN)

Consider first the case in which STN is supposed to contain discrete channel populations. This is consistent with evidence for somatotopy in STN (DeLong et al. 1985) and places STN on the same footing as the other basal ganglia nuclei in the model. There are then three contributions to the equilibrium activation $\tilde{a}_i^+$ of the ith channel of STN. The first component is the afferent input to basal ganglia for channel i. The STN, lacking the sophisticated pattern matching apparatus of the medium spiny cells, may not be able to veridically extract the salience c_i. However, the computed afferent signal on any channel may be modelled as the salience value with an additive, channel dependent noise term.

Then, given that STN projections are summed by the target nuclei – the globus pallidus internal segment (GPi) and the substantia nigra reticulata area (SNr), and the globus pallidus external segment (GPe) and, assuming the expectation of the noise is zero, the overall contribution of the noise becomes insignificant for a realistically large number of channels. We therefore drop the noise terms from subsequent expressions to simplify the working. We now consider separately the potentially active channels (those in P) and those which are not. For the former, we write the contribution to STN activity from external input to basal ganglia as $w_t c_i$, where w_t governs the synaptic strength of afferents to STN. Non-members of P are all those afferents to basal ganglia which were not selected in local striatal competitions. We assume that these contributions to STN activity may be modelled as a mean value, plus additive noise. Once again, assuming the noise has zero expectation and that the summed value of this non-active input is approximately constant, we can represent this by a positive constant contribution ϵ', per channel. This low level 'background' of cortical input to STN will help sustain the observed tonic output in this nucleus (Delong et al. 1985; Wichmann et al. 1994). The tonic level may, of course, also contain a contribution due to the intrinsic membrane properties of cells in STN. However, this is of no consequence for the nucleus as a whole at the functional architectural level, and we therefore absorb any such contribution into ϵ. Finally there is a component $w_g y_i^e$, from the ith channel of GPe, where y_i^e is its output, and w_g is the synaptic weight between GPe and STN. Combining all three components, we have $\tilde{a}_i^+ = w_t c_i + \epsilon' - w_g y_i^e$. If the output of the ith channel in STN is x_i^+ and m^+ is the gradient on the strictly increasing part of the output function, then $x_i^+ = m^+ \tilde{a}_i^+ H(\tilde{a}_i^+)$. The STN target nuclei are then innervated by a total excitation

$$X^+ = m^+ \sum_{i=1}^{n} (w_t c_i + \epsilon' - w_g y_i^e) H(\tilde{a}_i^+) \tag{9}$$

Given the relatively small size of STN and the possibility of massive intra-nucleus excitation (Kita et al. 1983), it is possible that STN does not support discrete channels. Instead, it may be more appropriate to consider a model in which all channels are served by a single cell population with output x^+ where

$$x^+ = m^+ \sum_{i=1}^{n} (w_t c_i + \epsilon' - w_g y_i^e) \tag{10}$$

Comparison of (9) and (10) shows that, in spite of their structural dissimilarity, both the discrete and homogeneous STN alternatives offer similar function with respect to the STN targets – namely, an integration of basal ganglia input and its redistribution in the form of diffuse excitation. Both models have been analysed and simulated but show little difference in their general patterns of behaviour. The model is therefore robust under variations in mechanisms of STN input integration and so we report only the results for the case of discrete channels.

2.4 GPe

Let the synaptic strengths with striatum and STN be w^- and w^+ respectively, and put $w^+ = \delta w^-$. Let $\tilde{a}_i^e$ be the equilibrium activation of channel i in GPe, and ϵ_e a channel independent threshold term, then $\tilde{a}_i^e = w^-(\delta X^+ - x_i^{e-}) + \epsilon_e$. Using the expression for x_i^{e-} given in (7)

$$\tilde{a}_i^e = w^- \left\{ \delta X^+ - m^- [(1-\lambda_e) w_s c_i - \epsilon] H_i^{\uparrow}(\lambda_e) \right\} + \epsilon_e \tag{11}$$

and the output relation is

$$y_i^e = m^e \tilde{a}_i^e H(a_i^e) \tag{12}$$

2.5 GPi/SNr

STN input to GPi/SNr is assumed to be the same as that for GPe. This is consistent with the evidence for branched STN collaterals to these areas (Deniau et al. 1978; Kita et al. 1983). Further, we suppose that afferents from STN have the same synaptic strength as they do at GPe. If w_e is the synaptic strength of afferents from GPe and ϵ_g the threshold term then, the GPi/SNr equilibrium activation is

$$\tilde{a}_i^g = w^-(\delta X^+ - x_i^{g-}) - w_e y_i^e + \epsilon_g \tag{13}$$

Substituting for x_i^{g-} from (8)

$$\tilde{a}_i^g = w^-(\delta X^+ - m^- [w_s(1+\lambda_g) c_i - \epsilon] H_i^{\uparrow}(-\lambda_g)) \quad - w_e y_i^e + \epsilon_g \tag{14}$$

If y_i^g is the GPi/SNr output at equilibrium then $y_i^g = m^g \tilde{a}_i^g H(a_i^g)$.

3 Analytic results

This section summarises the most important analytic results. In working the solutions, it is convenient to normalise all output function gradients m to one; this simply implies a possible rescaling of the weights and threshold offsets. We first solve for the activity within each of the basal ganglia nuclei and go on to use these expressions to explore the selection properties of the model as a whole and its behaviour under dopaminergic modulation. Detailed proofs of all the results may be found in Gurney et al. (1998).

3.1 Nucleus activities

GPe. Let $\mathcal{Q}_0$ be the set of non-GPe-active channels (i.e. $\mathcal{Q}_0 = P - P_e^*$). Now define two subsets of P_e^* by $\mathcal{Q} = \{i \in P_e^* : y_i^e > 0\}, \mathcal{Q}^* = \{i \in P_e^* : y_i^e = 0\}$. Then

$$
\begin{aligned}
&i \in \mathscr{Q}_0 : y_i^e = w^- \delta X^+ + \epsilon_e \\
&i \in \mathscr{Q} : y_i^e = w^- \{\delta X^+ - [(1-\lambda_e) w_s c_i - \epsilon]\} + \epsilon_e \\
&i \in \mathscr{Q}^* : y_i^e = 0
\end{aligned} \tag{15}
$$

STN. Starting from (9) it is possible to determine parameter constraints by examining signal values under quiescent conditions, that is $c_i = 0,\ \forall i$. If $\hat{X}^+$ is the tonic STN level under these circumstances then, since $\hat{X}^+ > 0$, $H(\tilde{a}_i) = 1,\ \forall i$ and (under gradient normalisation) (9) gives $\hat{X}^+ = n(\epsilon' - w_g y_i^e)$. All channels are members of $\mathscr{Q}_0$ so that, substituting from (15) and solving for $\hat{X}^+$ gives $\hat{X}^+ = n(\epsilon' - w_g \epsilon_e)/(1 + n w_g \delta w^-)$. For this to be positive requires

$$
\epsilon' > w_g \epsilon_e \tag{16}
$$

For general input conditions, if S^* is the set of channels for which $H(\tilde{a}_i^+) = 1$ then

$$
X^+ = \sum_{i \in S^*} (w_t c_i + \epsilon' - w_g y_i^e) \tag{17}
$$

We now show by *reductio ad absurdum* that S^* can never be empty. Suppose $S^* = 0$, so that $X^+ = 0$. Then from (15), $y_i^e \le \epsilon_e\ \forall i$, so that $\epsilon' - w_g y_i^e \ge \epsilon' - w_g \epsilon_e > 0$, where the last inequality is ensured by (16), implying $\tilde{a}_i^+ > 0\ \forall i$. Therefore $X^+ > 0$ and $S^* \neq 0$. Thus, the original premise ($S^* = 0$) is contradicted and is therefore false.

We now solve for X^+. Splitting the summation in (17) over subsets determined by the GPe output classes gives

$$
X^+ = \sum_{i \in S^*} (w_t c_i + \epsilon') - w_g \left(\sum_{i \in S^* \cap \mathscr{Q}_0} y_i^e + \sum_{i \in S^* \cap \mathscr{Q}} y_i^e \right) \tag{18}
$$

Now define $n^s = |S^*|, \phi_s^q = |S^* \cap \mathscr{Q}|/n^s$. Put $\mathscr{M} = \mathscr{Q} \cap \mathscr{Q}_0$ and $\phi_s^m = |S^* \cap \mathscr{M}|/n^s$. Define the mean salience values

$$
\langle c \rangle_s = \frac{1}{n^s} \sum_{i \in S^*} c_i \qquad \langle c \rangle_{q,s} = \frac{1}{n^s \phi_s^q} \sum_{i \in S^* \cap \mathscr{Q}} c_i \tag{19}
$$

Then, substituting in (18) from (15) and solving for X^+ gives

$$
\begin{aligned}
X^+ = \frac{n^s}{1 + \delta w_g w^- n^s \phi_s^m} \Big\{ & w_t \langle c \rangle_s + w_g w^- \\
& \times \phi_s^q [(1-\lambda_e) w_s \langle c \rangle_{q,s} - \epsilon] + \epsilon' - w_g \phi_s^m \epsilon_e \Big\}
\end{aligned} \tag{20}
$$

GPi/SNr. The general expression for GPi/SNr activation is given by (14). The tonic state, with activation $\hat{a}^g$, occurs when $i \notin P^*$ and $i \in \mathscr{Q}_0$. Then

$$
\hat{a}^g = w^- \delta X^+ \gamma^e - w^e \epsilon_e + \epsilon_g \tag{21}
$$

where $\gamma^e = (1 - w^e)$. The right hand side of (21) must be greater than zero for a positive tonic level. Thus, assuming ϵ_g and ϵ_e are of similar magnitude, then $\gamma^e > 0$ which implies

$$
w^e < 1 \tag{22}
$$

3.2 The basal ganglia as a selection mechanism

This section demonstrates the main analytic results concerning the fundamental selection properties of the model. We first show that the model satisfies the minimal requirement of implementing an order-preserving mapping; this was the definition of a selection mechanism given in GPR1. Next, we show that the model exhibits features to facilitate potentially useful selection; automatic capacity scaling competitiveness, and the promotion of selectivity.

3.2.1 Order-preserving mapping. The model is a selection mechanism in the sense defined in GPR1 if it implements an order-preserving mapping and is endowed with selection thresholds θ_1 and θ_2 that define the selected and non-selected sets of output signals S and $\bar{S}$, respectively ($y_i^g \in S$ if $y_i^g < \theta_1$ and $y_i^g \in \bar{S}$ if $y_i^g > \theta_2$). Further, given that the tonic output $\hat{y}^g$ should be sufficient to ensure non-selection we suppose that $0 \le \theta_1 < \theta_2 \le \hat{y}^g$.

If $\Delta_{ij} y^g = y_i^g - y_j^g$, then signal ordering is preserved if $c_j > c_i \Rightarrow \Delta_{ij} y^g \ge 0$. To prove this it is easier to work initially with the activation. If $\Delta_{ij} \tilde{a}^g = \tilde{a}_i^g - \tilde{a}_j^g$, then from (13)

$$
\begin{aligned}
\Delta_{ij} \tilde{a}^g = w^- \Big\{ & [(1+\lambda_g) w_s c_j - \epsilon] H_j^{\uparrow}(-\lambda_g) \\
& - [(1+\lambda_g) w_s c_i - \epsilon] H_i^{\uparrow}(-\lambda_g) \Big\} - w_e \Delta_{ij} y^e
\end{aligned} \tag{23}
$$

Here, $\Delta_{ij} y^e = y_i^e - y_j^e$ and is defined using (15) and by making the appropriate assignments for i, j as members of $\mathscr{Q}_0, \mathscr{Q}$ and $\mathscr{Q}^*$. In a similar way the step functions $H_j^{\uparrow}(-\lambda_g), H_i^{\uparrow}(-\lambda_g)$ are defined according to whether $i, j \in P^*$. These combinations of set membership yield ten categories in all and examination of each case gives the following result: if $c_j > c_i$, then $\Delta_{ij} \tilde{a}^g \ge 0$, with equality holding if and only if $i, j \notin P^*$. Using the output relation (3), $\Delta_{ij} \tilde{a}^g > 0 \Rightarrow y_i^g > y_j^g$ unless $y_i^g = y_j^g = 0$, and so we have

Result 1: $\Delta_{ij} y^g \ge 0$ with equality holding if and only if $y_i^g = y_j^g = 0$ or $i, j \notin P^*$

3.2.2 Capacity scaling. This is discussed in GPR1 and refers to the requirement that there must be a suitable balance between excitation and inhibition to enable the set of selected channels to be non-empty. To investigate this, we need to determine the general behaviour of channel output activity $\tilde{a}_i^g$ with respect to the tonic level $\hat{a}^g$. If $\Delta^{\hat{i}} = \tilde{a}_i^g - \hat{a}^g$, then using (14) and (21), it is possible to write a general form for $\Delta^{\hat{i}}$ which accommodates all cases

$$
\Delta^{\hat{i}} = \delta \Delta X^+ - L(\lambda_g, \lambda_e) c_i + k_3 \tag{24}
$$

where $\Delta X^+ = k_1 X^+ - k_2 \hat{X}^+$ and is positive since $k_1 \ge k_2$. Further, the k_i and L do not depend on the number of channels; the only salience-dependent terms are X^+ and c_i and the dopamine dependence is contained within L.

Consider now what would happen if there were no inhibition from GPe to STN, that is $w_g = 0$. Then $n^s = n$ and, from (20), $X^+ = n(w_t\langle c\rangle_s + \epsilon')$ and $\hat{X}^+ = n\epsilon$. Thus, ΔX^+ is proportional to n, the excitatory term $\delta\Delta X^+$ dominates in (24), and capacity scaling may only be achieved by ensuring $\delta = O(1/n)$.

Now consider the case when GPe inhibition is instantiated. We first show that X^+ is bounded above. With reference to (20), the factor in the curly brackets on the right hand side contains terms whose magnitude is limited by the scale of the weights and is therefore bounded above by some value c_0 and

$$X^+ \leq n^s c_0/(1 + \delta w_g w^- n^s \phi_s^m) \tag{25}$$

This is not necessarily bounded above since n^s may grow indefinitely while $n^s\phi_s^m$ remains bounded. To show that this cannot occur, we first observe that – for sufficiently large X^+ – all $y_i^e > 0$ (see Eq. 11). Formally, $\exists X_*^+$ such that

$$X^+ > X_*^+ \Rightarrow y_i^e > 0\ \forall i\ \Rightarrow \mathcal{Q}^* = 0 \Rightarrow \phi_s^m = 1 \tag{26}$$

We now proceed by *reductio ad absurdum*. Thus, suppose that X^+ is not bounded above, then given any N, $\exists n^s > N$ such that

$$X^+ > \max(X_*^+, c_0/\delta w_g w^-) \tag{27}$$

so that (26) holds and $\phi_s^m = 1$. Then, from (25), $X^+ \leq c_0/(1/n^s + \delta w_g w^-) < c_0/\delta w_g w^-$ which contradicts (27) and so X^+ is bounded above. It follows immediately that, so too is ΔX^+. Therefore, the excitatory term $\delta\Delta X^+$ is bounded without making δ indefinitely small and matching it precisely to the channel capacity. Further, one corollary of the boundedness of X^+ and (25) is that ϕ_s^m is bounded below. In summary, we have the following result

Result 2:

1. If $w_g = 0$ capacity scaling may only be achieved by ensuring that $\delta = O(1/n)$.
2. If $w_g \neq 0$, X^+ is bounded above and $\exists\delta_0 > 0$, such that if $\delta > \delta_0$, capacity scaling is maintained as $n \to \infty$.
3. ϕ_s^m is bounded below.

The reason for the limiting of X^+ is, of course, the GPe inhibition of STN. This manifests itself in the term $\delta w_g w^- n^s \phi_s^m$ in the denominator of the expression for X^+ in (20), which was crucial in our proof of the boundedness of X^+. The capacity scaling in the model is therefore *automatic* in the sense that it is obtained by the dynamics of the GPe $\rightarrow$ STN inhibitory feedback interaction, and is not determined *structurally* by explicitly setting a weight value as such.

3.2.3 Competitiveness. The model retains the competitiveness displayed by the simple feedforward mechanisms discussed in GPR1 as may be demonstrated by evaluating $d\tilde{a}_i^g/dc_j$. Once again there are a set of cases based on set membership of i with respect to $P^*, \mathcal{Q}_0, \mathcal{Q}$ and $\mathcal{Q}^*$ giving the following result

Result 3:

1. If $i \neq j$ then $\mathrm{d}\tilde{a}_i^g/\mathrm{d}c_j > 0$ if $i \in S^*$, $\mathrm{d}\tilde{a}_i^g/\mathrm{d}c_j = 0$ if $i \notin S^*$.
2. If $i \notin S^*$ then $\mathrm{d}\tilde{a}_i^g/\mathrm{d}c_i < 0$ unless $i \notin P^*$, in which case $\mathrm{d}\tilde{a}_i^g/\mathrm{d}c_i = 0$.
3. If $i \in S^*$ then if $\delta < 1$ and $w_t = w_s$, $\mathrm{d}\tilde{a}_i^g/\mathrm{d}c_i < 0$ unless $i \notin P^*$, in which case $\mathrm{d}\tilde{a}_i^g/\mathrm{d}c_i > 0$.

A corollary is that a similar set of results hold for the output y_i^g so long as $y_i^g \neq 0$. Part 1 of Result 3 states that there may be an increase in GPi/SNr excitation under external basal ganglia stimulus. This is consistent with known properties of GPi/SNr (Mink 1996) and occurs in the model on channels $j \neq i$ when channel i becomes increasingly salient. Its origin is the excitation via STN that channels other than i receive when c_i is increased. If c_i is sufficiently large, it may be possible for channel i to become selected and for the output on a previously selected channel k to be raised to the point where it loses its selected status; in this case we say that channel i has interrupted channel k. Parts 2 and 3 of Result 3 state that, in general, the output activity on a channel tends to decrease with increased salience on that channel. The exception occurs when the salience is insufficient to make the channel striatally active. Then, STN excitation grows with no commensurate striatal inhibition so that the output activity increases.

3.2.4 Selectivity. Consider again the change in GPi/SNr activation given by (24). Suppose that the salience on channel k is fixed while that on other channels is allowed to increase. Then by result (3), X^+ – and thereby ΔX^+ – will increase. Thus, the activity of other channels makes any reduction in output $\Delta^k < 0$ on channel i harder to achieve. This is, of course, just a result of the inter-channel competition and it will tend to limit the promiscuity (equivalently increase the selectivity) of the model.

The degree of selectivity enhancement will depend on the rate at which salience increase affects the total excitatory term $\delta\Delta X^+$ in (24). Now $\mathrm{d}(\delta\Delta X^+)/\mathrm{d}c_i$ is proportional to $\delta\mathrm{d}X^+/\mathrm{d}c_i$. To determine the latter, let $\chi_s(i)$ and $\chi_q(i)$ be characteristic functions for membership of S^* and $\mathcal{Q}$, respectively ($\chi_s(i) = 1$ iff $i \in S^*$, $\chi_q(i) = 1$ iff $i \in \mathcal{Q}$). From (19)

$$\frac{\mathrm{d}\langle c\rangle_s}{\mathrm{d}c_i} = \frac{\chi_s(i)}{n^s} \qquad \frac{\mathrm{d}\langle c\rangle_{q,s}}{\mathrm{d}c_i} = \frac{\chi_s(i)\chi_q(i)}{n^s\phi_s^q} \tag{28}$$

and using (20)

$$\frac{\mathrm{d}X^+}{\mathrm{d}c_i} = \frac{\chi^s(i)[w_t + w_g w^-(1-\lambda_e)w_s\chi_q(i)]}{1 + \delta w_g w^- n^s \phi_s^m} \tag{29}$$

Now suppose $\chi_s(i) = 1$. Further, if $w_t = w_s$ (as assumed in Result 3, Part 3) then (29) implies

$$\frac{dX^+}{dc_i} = \frac{w_t[1 + w_g w^-(1-\lambda_e)\chi_q(i)]}{1 + \delta w_g w^- n^s \phi_s^m} \quad (30)$$

For large n_s, Result 2, Part 3 implies $n^s\phi_s^m \gg 1$, so that

$$\frac{dX^+}{dc_i} \approx \frac{w_t[1 + w_g w^-(1-\lambda_e)\chi_q(i)]}{\delta w_g w^- n^s \phi_s^m} \geq \frac{1}{w_g w^-}\frac{w_t}{n} \quad (31)$$

Now, under gradient normalisation, the maximum activation should not be significantly larger than 1 if the linear portion of the neuron output function is to be exercised under most input combinations. The same applies to the excitatory and inhibitory contributions to each node and, since there are only single inhibitory inputs to each node, this places a similar constraint on w^- and w_g. Weights which obey this criterion will be said to be *unit scaled*. In particular, if $w_g w^- = 1$, (31) gives

$$\delta\frac{dX^+}{dc_i} \geq \frac{w_t}{n} \quad (32)$$

Now suppose there is no GPe → STN pathway, so that $w_g = 0$. Then $n^s = n$, and if $\delta = 1/n$ (to obtain capacity scaling) then (30)

$$\delta\frac{dX^+}{dc_i} = \frac{w_t}{n} \quad (33)$$

Comparison with (32) shows that a more rapid increase in excitation occurs with the GPe → STN pathway instantiated. This, in turn, implies more pronounced competitiveness and enhanced selectivity.

3.3 Dopaminergic modulation

In this section we examine the way in which the GPi/SNr output changes with levels of dopamine in the selection and control pathways parameterised by λ_g and λ_e, respectively. The result for the selection pathway follows immediately from (14). Thus, if $i \in P^*$

$$\frac{d\tilde{a}_i^g}{d\lambda_g} = -w^- w_s c_i \quad (34)$$

To find $d\tilde{a}_i^g/d\lambda_e$ necessitates the evaluation of $dX^+/d\lambda_e$. From (20)

$$\frac{dX^+}{d\lambda_e} = \frac{-n^s w_g w^- w_s \phi_s^q \langle c\rangle_{q,s}}{1 + \delta w_g w^- n^s \phi_s^m} \quad (35)$$

A complete analysis requires the examination of several cases but notice that $\langle c\rangle_{q,s}$ must be non-zero for $\tilde{a}_i^g$ to depend on λ_e. Combining the results obtained from (35) with (34) gives

Result 4:

$$\frac{d\tilde{a}_i^g}{d\lambda_g} \quad \begin{cases} < 0 : i \in P^* \\ = 0 : i \notin P^* \end{cases} \quad (36)$$

$$\frac{d\tilde{a}_i^g}{d\lambda_e} \quad \begin{cases} < 0 : \langle c\rangle_{q,s} \neq 0 \\ = 0 : \langle c\rangle_{q,s} = 0 \end{cases} \quad (37)$$

Since y_i^g is a monotonic function of $\tilde{a}_i^g$, there is a corollary of this result for GPi/SNr output in which the condition for a non-zero derivative is extended to include $y_i^g \neq 0$. The general effect of increasing levels of dopamine in *either* pathway is, therefore, to depress GPi/SNr output levels thereby making selection more promiscuous.

Dopaminergic modulation in the control pathway is mediated by efferents of GPe to both STN and GPi/SNr. However, the GPe → GPi/SNr pathway is crucial for the control of the inter-signal interval $\Delta_{ij}\tilde{a}^g$, for it may be shown that $d\Delta_{ij}\tilde{a}^g/d\lambda_e \neq 0$ only if $w_e \neq 0$. Further, the interval $\Delta_{ij}\tilde{a}^g$ increases under most circumstances with increasing dopamine levels.

4 Simulation results

4.1 Parameter details

Simulations made use of a 6-channel model. All slope parameters (m^-, m^+, m^e, m^g) were set to 1, which is the gradient normalisation assumption made in the analysis. Unit scaling of the weights applied to w_s, w_t, w^- and w_g, which were all set equal to 1. Result 3 also requires $\delta < 1$; we used $\delta = 0.9$ so that $w^+ = \delta w^- = 0.9$. To satisfy the condition in (22), w_e was set to 0.3. The striatal offset ϵ was set to 0.2 to force a 'down-state' unless the activation is positive. The other offsets $\epsilon'\epsilon_e$ and ϵ_g were set to the negative values $-0.25, -0.2$ and -0.2, respectively, to maintain tonic rates. In particular, the tonic output of GPi/SNr, $\hat{y}^g$, was approximately 0.15. Given that $0 < y^g < 1$ and the tonic output of GPi/SNr is approximately 60–80 Hz in primates (Georgopoulos et al. 1983; Mink and Thach 1991) this implies a physiologically plausible maximum GPi/SNr rate of 400–500 Hz. Finally, the rate constant k in (1), which sets the time scale of the simulations, was 25.

4.2 Basic selection properties

Some of the properties described in Sect. 3.2 are illustrated in the simulation results shown in Fig. 2. In Fig. 2a, channels 1 and 2 were stimulated during the simulation, while the salience on the remaining channels was set to zero. Channel 3 is therefore representative of channels 3–6. The dopamine levels λ_e and λ_g were both set to 0.2. Initially there is zero salience on all six channels (note that the initial transients in the output signals are artifacts of the simulator as it establishes a consistent set of activity levels). At time $t = 1$, the salience on channel 1 is increased to 0.4. This results in decreased output y_1^g on this channel, and increased output on the other four channels. If $y_1^g < \theta_1$ then channel 1 has become selected. At $t = 2$, the salience of channel 2 becomes 0.6. This is sufficient to force $y_2^g = 0$,

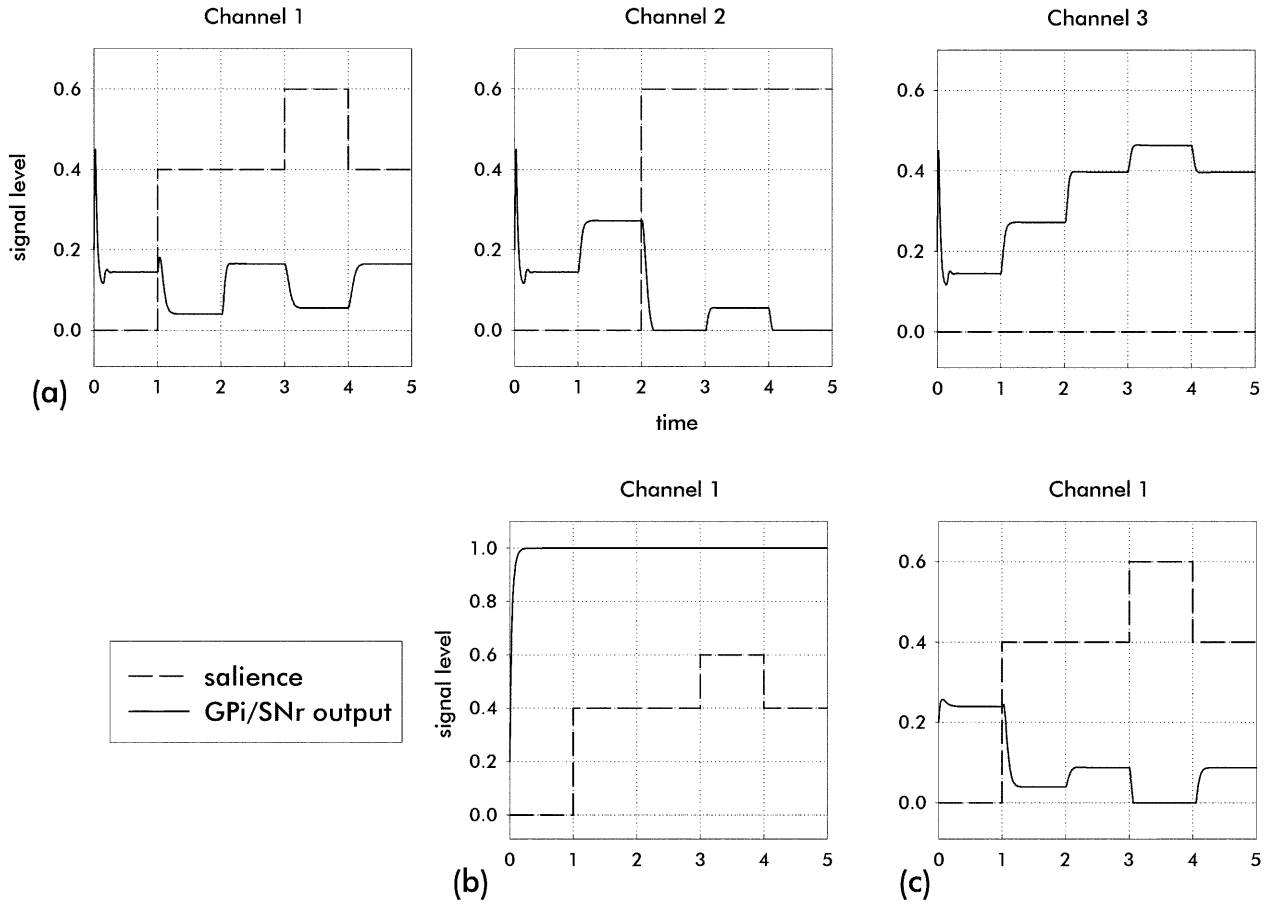

Fig. 2a–c. Simulation results for three channels in a 6-channel model. Only channels 1 and 2 have non-zero salience; channel 3 is shown as representative of the other, non-active channels. For each channel, the *solid line* indicates the GPi/SNr output and the *dashed line* the input salience. Time is measured in arbitrary units. **a** Results for an intact model with synaptic weights on STN efferents having 0.9 times the value of those from striatum. **b** The result of 'lesioning' the model GPe → STN pathway while maintaining the synaptic weights from STN at their former values. **c** The same lesion as in **b** but now the weights from STN are 1/6 of their former values

thereby ensuring selection of channel 2, while pushing y_1^g above the tonic value $\hat{y}^g$. The output on channel 3 (and all other non-active channels) is increased still further. Thus, if channel 1 were selected prior to $t = 2$, the selection of channel 2 has caused the interruption of its selection. The next two events are initiated by a transient increase in salience on channel 1 from $t = 3$ to $t = 4$. During this time, both channels 1 and 2 have the same, comparatively high salience, but inter-channel competition leads to a higher common output level than would be seen with the same salience on a single channel in isolation. Note that the ordering of signals is preserved throughout: if $c_i > c_j$ then $y_i^g \leq y_j^g$.

Figure 2b demonstrates the phenomenon of capacity scaling. The results were obtained using a model in which the GPe → STN pathway had been lesioned while the weights associated with STN afferents remained unchanged. The salience events were identical to those used to obtain Fig. 2a, but only channel 1 is shown. The output saturates at 1 throughout the stimulus period and no selection is possible. Selection may be reinstated by setting $\delta = 1/n = 1/6$, as shown in Fig. 2c. However, to retain this behaviour as n is increased, δ must be decreased in proportion. Comparison of the graph for channel 1 in Fig. 2a and c also demonstrates the reduction in selectivity with no GPe → STN pathway. Thus, in the latter case both channels are able to become selected for $3 < t < 4$, whereas their selection is uncertain under GPe inhibition of STN.

4.3 Dopaminergic modulation

Figure 3a shows a simulation for channel 1 using the sequence of salience events used to obtain the results in Fig. 2. With no dopamine ($\lambda_g = \lambda_e = 0$), selection does not occur. With an intermediate level of dopamine in the selection pathway but none in the control pathway ($\lambda_g = 0.2, \lambda_e = 0$), the GPi/SNr output signals are somewhat reduced. The same applies with dopamine in only the control pathway ($\lambda_g = 0, \lambda_e = 0.2$), but the effect is less pronounced. With equal dopamine levels in both pathways, the effects on GPi/SNr from each pathway are combined synergistically.

One consequence of the dopamine-related reduction in channel output is that selection within the model tends to be more promiscuous. This is illustrated in

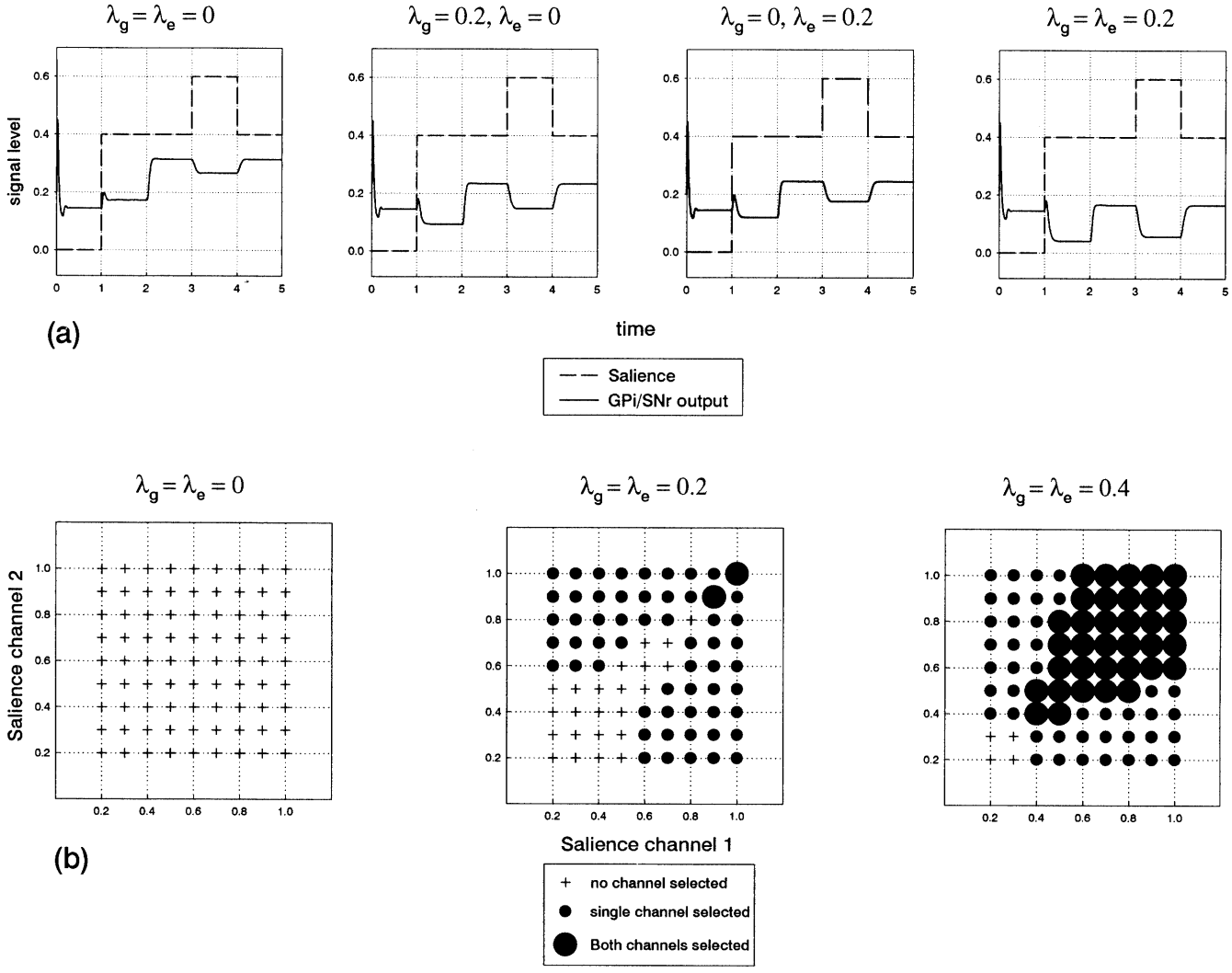

Fig. 3a,b. The effect of dopamine on model output behaviour. **a** A simulation similar to that which formed the basis of the results in Fig. 3 (only channel 1 is shown here). **b** The effect of dopamine on selection with two competing channels. Each panel shows channel selection over a range of salience combinations, with salience taking values between 0.2 and 1 in steps of 0.1. In each case, a channel is deemed as selected if it has zero output. Dopamine levels in both pathways were the same

Fig. 3b in which each panel shows selection across two competing channels over a range of salience combinations, taking values between 0.2 and 1 in steps of 0.1. In each case, a channel is deemed as 'selected' if it has zero output and dopamine levels in both control and selection pathways are the same. With no dopamine, neither channel ever gets selected no matter how large the salience values. Now consider the case of an intermediate level of dopamine ($\lambda_g = \lambda_e = 0.2$). Here, saliences below 0.6 fail to initiate selection but, for values greater than or equal to this, channel selection is possible. With closely matched salience values less than 0.9, the inter-channel competition is equally closely matched and neither channel is selected. However, if both channels are sufficiently salient, they may force simultaneous selection. Turning to the case of high dopamine ($\lambda_g = \lambda_e = 0.4$) a similar general pattern of results occurs but the salience threshold for selection is smaller (0.4) and there is significantly more opportunity for simultaneous channel selection.

4.4 Comparison with neurophysiological data

One powerful test of a model is to compare its characteristic signal profiles under external stimulation with those obtained under similar conditions in biological systems. Signal profiles may be thought of as signatures of structural features associated with their generation so that their identification, both in vivo and in the model, is evidence for a common architecture. This stance is similar to that adopted in systems (control) theory where structural and/or parametric identification of a system is made possible by examining its response to stereotypical inputs. In particular, a system is completely characterised by its 'impulse response': its output after being driven by a pulsed input with very short (theoretically zero) duration and very large (theoretically infinite) amplitude. Artificial electrical stimulation of neural tissue by a microelectrode typically results in this kind of input. Ryan and Clark (1991) used this technique with short (0.2 ms)

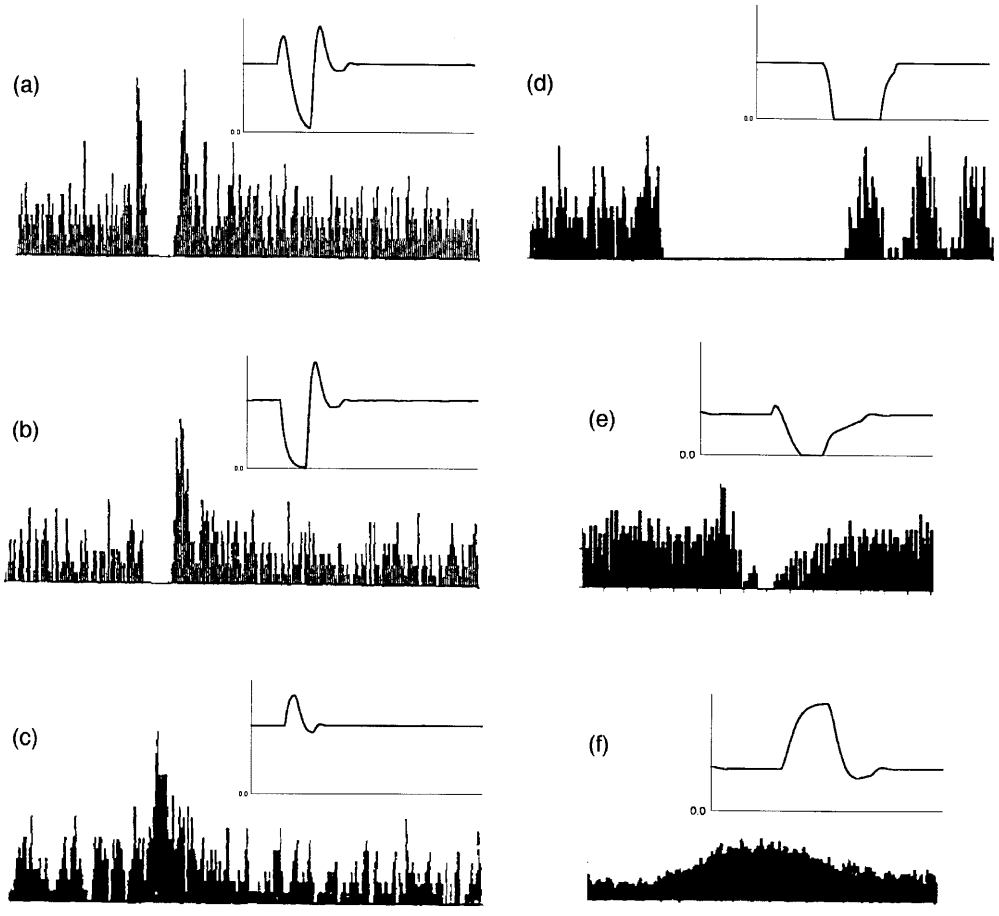

Fig. 4a–f. Single-unit recordings (peristimulus histograms) and corresponding model simulation results (*line graphs*). **a–c** Responses of pallidal units in the rat following single-pulse electrical stimulation of cortical input to the basal ganglia (Ryan and Clark 1991; figures reproduced with permission of Springer-Verlag). The simulations all use rectangular salience pulses of short duration (relative to the model's intrinsic time scale) and large amplitudes (> 1). **d** Data and simulation following the lesion of excitatory input from STN. **e** Cells in monkey SNr displaying disinhibition during a behavioural task (Schultz 1986; figures reproduced with permission of the American Physiological Society) and model GPi/SNr output for a single salient channel. **f** Data for an SNr neuron from the same experiment which increases its output together with a corresponding simulation result from a non-stimulated channel

pulses of large amplitude current (0.3, 0.7 mA) to stimulate rat cortex and then record from GPe. Some of the data they obtained are shown in Fig. 4a–c.

These recordings display transients of increased and decreased activity in various combinations commensurate with short periods of excitation and inhibition. The inset in each panel shows the simulated output from GPe obtained using a salience pulse of short duration (relative to the model's intrinsic time scale) and large amplitude (greater than or equal to 1). Comparison with the electrophysiological data is made possible by interpreting the model output as the mean firing rate of GPe; in each case the pattern of excitatory and inhibitory transients is similar. Figure 4d shows data for the same signal injection site as that shown in Fig. 4a, but following the disabling of excitatory input from STN; the inset shows the corresponding model simulation. Notice the reduction in early and re-bound excitation and increased duration of the inhibitory phase in both data and simulation. As well as examining the response of the system to artificial pulses, it is also necessary to confirm that the model can exhibit signal behaviour in its normal operating regime which is comparable to data available from behaving animals. Figure 4e shows data from cells in monkey SNr displaying reduction in activity during a behavioural task (Schultz 1986). The inset in this panel is the model GPi/SNr output for a single active channel using a small amplitude, rectangular pulse input. The primary point illustrated by the data is the fundamental process of disinhibition in SNr but, bearing in mind a cautionary note that the biological salience may not have the simple rectangular form used in the simulation, it is intriguing to observe other points of contact between data and simulation. Thus, the rise time of the SNr signal is substantially slower than that of its initial fall, and the disinhibition onset is preceded by a short excitatory transient. Figure 4f shows an SNr neuron from the same experiment which increases its output, together with a comparable simulation result from a non-stimulated channel. We would predict from our model, therefore, that the data in Fig. 4e and f are associated with active and non-active channels respectively for the behavioural task employed.

5 Discussion

5.1 Functional mechanisms of the basal ganglia architecture

We have shown that a computational model based on essential features of basal ganglia anatomy can deliver GPi/SNr output signals consistent with the function of action selection. Signals are selected in two stages. First, a set of topographically local recurrent circuits within the striatum perform hard switching to enable, at most,

a single channel to be available for further processing within each such circuit. Next a global feedforward network based on an off-centre on-surround architecture selects from the winners of the local circuit competitions. This second stage of selection satisfies the formal requirement of an order-preserving mapping between input (channel salience) and output (GPi/SNr inhibition). Further, while allowing multiple channel selection (soft switching), it is endowed with inter-channel competition that can potentially limit the promiscuity of selection.

The properties of the global selection pathway are modulated by control signals from GPe and the role of the putative control pathway appears to be three-fold. First, to ensure that there is an appropriate balance between excitation and inhibition that enables useful selection to occur. This process of capacity scaling is performed automatically using the negative feedback from GPe to STN and is independent of the number of active STN channels n^s. The use of negative feedback to stabilise a system or adaptively control its operating point is a familiar concept in control engineering, and it should not be surprising that such mechanisms occur naturally in living systems especially in control structures such as the basal ganglia. We contend that it is unrealistic to suppose that the synaptic contacts with STN (governed by δ) are tailored to a global system parameter such as the number of channels. We propose instead that the basal ganglia use the adaptive mechanism supplied by negative feedback from GPe to STN to auto-scale the excitation from STN to accommodate an arbitrary number of channels. The second role of the control pathway is to enhance the selectivity under inter-channel competition. This may also be viewed as another feature of the dynamic assignment of excitation in the model that also underlies capacity scaling. Third, this pathway aids the expression of dopaminergic control of selection and, in general, dopamine in the selection and control pathways works synergistically to promote more promiscuous selection and to increase the inter-channel output activation interval.

5.2 Relation to clinical, behavioural and physiological studies

The synergistic effect of dopamine in both selection and control pathways is consistent with the study of Murer et al. (1997), which showed that the concurrent activation of both dopamine receptor sub-types had a mutually facilitating effect on SNr firing rate. With low levels of dopamine, selection is prohibited under a wide range of saliences. The behaviour of the model under these circumstances is consistent with the observed relationship between dopamine depletion in humans and several symptoms of Parkinson's disease (PD). These include bradykinesia (the slowness of movement execution) and hypokinesia (the poverty of spontaneous movements, e.g. a relative absence of facial movements, blinking and arm swinging when walking (Korczyn 1995)). In PD these two symptoms are often subsumed under the heading of akinesia (absence of movement) but, whichever terminology is used, they can be viewed as deficiencies in the ability to select and execute motor actions. In terms of our model, Parkinson's patients would be unable to release appropriately the tonic inhibitory output of GPi/SNr on selected motor channels; thus hypokinesia would then be consistent with the failure of the current model to select a channel. However, for models to be able to address the issue of bradykinesia (slowing of selected movements), a link between the degree of disinhibition and the rate of movement is needed. Such a mechanism has been successfully used in a biologically inspired model of motor control (Bullock et al. 1998) and is the basis for the gating of motor plant in our embodied model of action selection (Gonzalez et al. 2000). Our model offers a similar explanation for the akinesia seen after dopamine-depleting lesions in animals (e.g. Jenner et al. 1984).

In our model we found that, with intermediate levels of dopamine, selection limiting in the model can force two highly salient channels to oppose each other, resulting in both being more weakly selected (less release of inhibition) than they would be if only one was present with the same salience. This corresponds to a situation in which two actions are performed simultaneously. In general, the performance of both tasks is poorer than that when each is conducted individually. Explanations for this often take the form of limited attention, but the term 'attention' has many strands (Styles 1997) and it is possible that one of these concerns the limitations imposed by competition within the basal ganglia. This possibility is supported by evidence from work by Benecke et al. (1986), which shows that the performance of PD patients (relative to controls) on dual motor tasks is worse than that extrapolated from their performance on the tasks individually. This would point to basal ganglia deficit rather than a cortical attention 'bottleneck' or lack of 'executive' control.

As the dopamine level is increased beyond normal levels, our model predicts that the opportunity for simultaneous release of inhibition (and thereby channel selection) is also increased. However, it is possible that the simultaneous reduction of output on channels with small salience would be unstable when the current model is embedded in a wider anatomical context that includes cortex, thalamus and the motor resource. In such an extended model we anticipate that there could then be rapid switching between the two associated behaviours, rather than true simultaneous action selection. This may parallel the rapid behavioural and cognitive switching, and the inability to ignore distractors, as seen in several clinical conditions associated with disorders of the basal ganglia in which high levels of dopamine neurotransmission are implicated: these include attention deficit hyperactivity disorder (Swanson et al. 1998), Tourette's syndrome (Brito 1997), schizophrenia (Calabresi et al. 1997) and stimulant intoxication (Genova et al. 1997). Initial simulation work in our own lab with thalamo-cortico-striatal loops and populations of spiking neu-

rons indicates that rapid switching is indeed a possibility under low salience conditions.

Huntington's disease is another condition associated with basal ganglia pathology but, rather than being due to loss of dopamine innervation, it is attributed to medium spiny cell degeneration. Smith et al. (2000) have shown that Huntington's disease patients are unable to apply the required corrections to arm trajectories in a motor task, in spite of making initially accurate movements. Smith et al. conjectured that the basal ganglia may be involved in error correction via its modulation of thalamus. However, as noted by Lawrence (2000), it is possible that the observed motor errors are a side-effect of the main function of basal ganglia proposed here – that of selection.

Turning to the physiological data, the correspondence between model simulation data and certain basal ganglia neural signal 'signatures' allows for the possibility that some of these signals may be explained in terms of classical linear systems theory (by assuming operation of sub-nuclei over an approximately linear portion of their output regime). One example of this is the multiphasic (excitation, inhibition and rebound) responses observed for GPe in the data of Ryan and Clark (1991), which are typical of the impulse responses of damped feedback systems, and may be due to the recurrent circuit comprising STN and GPe. Further, a characteristic of low-order systems is the short duration of the early phase of the impulse response (compared to the longer decay component) which is evident in both the simulation and data of Fig. 4.

Closer inspection of Fig. 4d, however, indicates that some features of the biological data are not replicated in the simulation. Thus, after a period of inhibition when GPe is quiet, GPe resumes activity with a bursting pattern in the spike train. Burst firing may be associated with intrinsic membrane properties of a neuron and, in the basal ganglia, one prominent example is supplied by the interaction of calcium and potassium currents in STN (Beurrier et al. 1999). Clearly, these phenomena are not accommodated in our simple neural models. However, we have recently demonstrated that it is possible to model these currents phenomenologically (Humphries and Gurney 2000) and reproduce a substantial portion of the signal behaviour observed in the in vitro culture of STN and GPe studied by Plenz and Kital (1999). We anticipate that this (intermediate) level of neural modelling will prove extremely useful in supplementing insights gleaned from the systems-level model described here.

Our results (see Fig. 4f) are also consistent with the analysis of Mink (1996), who drew attention to the rarely emphasised – but often observed – increases in the firing rates of some output neurons in GPi/SNr which accompany the more commonly reported reduction in firing. The latter forms the basis of the fundamental process of disinhibition identified by Chevalier and Deniau (1990). We assume that these observations reflect the process of selection in our model where the output activity of selected channels is suppressed while that of competing, but non-selected channels is maintained or increased.

5.3 Conclusion

The model and analysis presented here shows, for the first time, that proposed selective functions for the basal ganglia Mink and Thach 1993; Hikosaka 1994; Redgrave et al. 1999a are confirmed features of a computational model of the biological architecture. Secondly, some properties of the model, such as capacity scaling and enhanced selectivity, are not apparent a priori and emerge only after quantitative analysis of the impact of the control pathway. These features provide hypotheses of an entirely different class to those generated by biological investigation alone. Finally, the process of selection is seen as a prerequisite to the process of combining a series of 'successful' selections into coordinated patterns of behaviour using reinforcement learning. It will be particularly interesting in the future to see how the current model can be integrated with recent proposals concerning reinforcement function (Schultz 1997; Redgrave et al. 1999b) and processes of sequence learning and automatisation (Hikosaka 1994; Jog et al. 1999).

References

Arbib M (1995) Introducing the neuron. In: Arbib M (ed) The handbook of brain theory and neural networks. MIT Press, Cambridge, Mass., pp 4–11

Benecke R, Rothwell J, Dick J, Day B, Marsden C (1986) Performance of simultaneous movements in patients with Parkinson's disease. Brain 109: 739–757

Beurrier C, Congar P, Bioulac M, Hammond C (1999) Subthalamic nucleus neurons switch from single spike-activity to burst-firing mode. J Neurosci 19: 599–609

Bouyer J, Park D, Joh T, Pickel V (1984) Chemical and structural analysis of the relation between cortical inputs and tyrosine hydroxylase-containing terminals in rat neostriatum. Brain Res 302: 267–275

Brito G (1997) A neurobiological model for Tourette syndrome centered on the nucleus accumbens. Med Hypotheses 49: 133–142

Bullock D, Cisek P, Grossberg S (1998) Cortical networks for control of voluntary arm movements under variable force conditions. Cereb Cortex 8: 48–62

Calabresi P, DeMurtas M, Bernardi G (1997) The neostriatum beyond the motor function: experimental and clinical evidence. Neurosci 78: 39–60

Chevalier G, Deniau J (1990) Disinhibition as a basic process in the expression of striatal functions. Trends Neurosci 13: 277–281

DeLong M, Crutcher MD, Georgopoulos A (1985) Primate globus pallidus and subthalamic nucleus: functional organization. J Neurophysiol 53: 530–543

Deniau J, Hammond C, Chevalier G, Feger J (1978) Evidence for branched subthalamic nucleus projections to substantia nigra, entopeduncular nucleus and globus pallidus. Neurosci Lett 9: 117–121

Genova L, Berke J, Hyman S (1997) Molecular adaptations to psychostimulants in striatal neurons: toward a pathophysiology of addiction. Neurobiol Dis 4: 239–246

Georgopoulos A, DeLong M, Crutcher MD (1983) Relation between parameters of step-tracking movements and single cell discharge in the globus pallidus and subthalamic nucleus of the behaving monkey. J Neurosci 3: 1586–1598

Gonzalez F, Prescott T, Gurney K, Humphreys M, Redgrave P (2000) An embedded model of action selection mechanisms in

the vertebrate brain. In: Proceedings of Society for Adaptive Behaviour Meeting, Paris, France, September 11–16, pp 157–166
Gurney K, Redgrave P, Prescott T (1998) Analysis and simulation of a model of intrinsic processing in the basal ganglia. Technical Report AIVRU 131, Dept Psychology, Sheffield University
Gurney K, Prescott TS, Redgrave P (2001) A computational model of action selection in the basal ganglia. I. A new functional anatomy. Biol Cybern 84: 401–410
Hikosaka O (1994) Role of basal ganglia in control of innate movements, learned behaviour and cognition. In: Percheron G, McKenzie J, Feger J (eds) The basal ganglia IV: new ideas and data on structure and function. Plenum, New York, pp 589–596
Humphries M, Gurney K (2000) A pulsed neural network model of bursting in the basal ganglia. Neural Networks. in press
Jenner P, Rupniak N, Rose S, Kelley E, Kilpatrick G, Lees A, Marsden C (1984) 1-methyl-4-phenyl-1,2,3,6-tetrahydropyridine-induced parkinsonism in the common marmoset. Neurosci Lett 50: 85–90
Jog M, Kuota Y, Connolly C, Hillegaart V, Graybiel A (1999) Building neural representations of habits. Science 286: 1745–1749
Kita H, Chang H, Kitai S (1983) The morphology of intracellularly labelled rat subthalamic nucleus: a light microscopic analysis. J Comp Neurol 215: 245–257
Korczyn A (1995) Parkinson's disease. In: Bloom F, Kupfer D (eds) Psychopharmacology: the fourth generation of progress. Raven, New York, pp 1479–1484
Lawrence A (2000) Error correction and the basal ganglia: similar computations for action, cognition and emotion? Trends Cogn Sci 4: 365–367
Mink J (1996) The basal ganglia: focused selection and inhibition of competing motor programs. Prog Neurobiol 50: 381–425
Mink J, Thach W (1991) Basal ganglia motor control. I. Nonexclusive relation of pallidal discharge to five movement modes. J Neurophysiol 65: 273–300
Mink J, Thach W (1993) Basal ganglia intrinsic circuits and their role in behaviour. Curr Opin Neurobiol 3: 950–957
Murer M, Riquelme L, Tseng K, Cristal A, Santos J, Pazo J (1997) D1-D2 dopamine receptor interaction: an in vivo single unit electrophysiological study. Neuroreport 8: 783–787
Plenz D, Kital ST (1999) A basal ganglia pacemaker formed by the subthalamic nucleus and external globus pallidus. Nature 400: 677–682
Redgrave P, Prescott T, Gurney K (1999a) The basal ganglia: a vertebrate solution to the selection problem? Neurosci 89: 1009–1023
Redgrave P, Prescott T, Gurney K (1999b) Is the short-latency dopamine response too short to signal reward error? Trends Neurosci 22: 146–151
Ryan L, Clark K (1991) The role of the subthalamic nucleus in the response of globus pallidus neurons to stimulation of the prelimbic and agranular frontal cortices in rats. Exp Brain Res 86: 641–651
Schultz W (1986) Activity of pars reticulata neurons of monkey substantia nigra in relation to motor, sensory, and complex events. J Neurophysiol 55: 660–677
Schultz W (1997) Dopamine neurons and their role in reward mechanisms. Curr Opin Neurobiol 7: 191–197
Schultz W, Romo R (1990) Dopamine neurons of the monkey midbrain: contingencies of responses to stimuli eliciting immediate behavioural reactions. J Neurophysiol 63: 607–624
Smith M, Brandt J, Shadmehr R (2000) Motor disorder in Huntington's disease begins as a dysfunction in error feedback control. Nature 403: 544–549
Styles E (1997) The psychology of attention. Psychology Press, East Sussex
Swanson J, Castellanos F, Murias M, LaHoste G, Kennedy J (1998) Cognitive neuroscience of attention deficit hyperactivity disorder and hyperkinetic disorder. Curr Opin Neurobiol 8: 263–271
Wichmann T, Bergman H, DeLong M (1994) The primate subthalamic nucleus. I. Functional properties in intact animals. J Neurophysiol 72: 494–506
Yamada W, Kock C, Adams P (1989) Multiple channels and calcium dynamics. In: Koch C, Segev I (eds) Methods in neuronal modelling. MIT Press, Cambridge, Mass., pp 97–134